

On the Connectedness of Nonlocal Minimal Surfaces in a Cylinder with (un)bounded Boundary Data

Mohamed Noah Abdel Wahab

Thesis for the attainment of the academic degree

Master of Science

at the TUM School of Computation, Information and Technology of the Technical University of Munich

Supervisor:

Prof. Dr. Marco Cicalese

Advisor:

Dr. Fumihiko Onoue

Submitted:

Munich, 16.05.2024

I hereby declare that this thesis is entirely the result of my own work except where otherwise indicated. I have only used the resources given in the list of references.

A handwritten signature in black ink, consisting of a stylized 'M' followed by a series of loops and a long horizontal stroke extending to the right.

Munich, 16.05.2024

Mohamed Noah Abdel Wahab

Abstract

Abstract

Nonlocal minimal surfaces confined within a cylinder exhibit unique behaviors dependent on external data. This thesis delves into these surfaces, which in contrast to classical minimal surfaces incorporate long-range spatial interactions. We consider a generalization of the model discussed in [8], a minimal surface confined within a cylinder with external data separated by a slab.

We demonstrate that for any external data separated by a slab containing symmetric parts of the cylinder, the minimal surface exhibits similar behavior as shown in [8]. Our results indicate that when the slab is wide, the minimal surface becomes disconnected from the data, while a narrow slab allows connection. This allows the behavior of similar models with symmetrically placed data to be predicted. Furthermore, the research demonstrates that for sufficiently narrow slabs, the surface “sticks” to the cylinder.

Finally, we present an example where the minimizer is completely disconnected from the external data, a phenomenon that is unique to nonlocal minimal surfaces. This work provides valuable insights into the behavior of these emerging mathematical objects and their interaction with external data.

Zusammenfassung

Nichtlokale Minimalflächen, die in einem Zylinder eingeschlossen sind, zeigen ein einzigartiges Verhalten, das von externen Daten abhängt. Diese Arbeit beschäftigt sich mit diesen Flächen, die im Vergleich zu klassischen Minimalflächen weitreichende räumliche Wechselwirkungen einbeziehen. Wir betrachten eine Verallgemeinerung des in [8] diskutierten Modells, einer in einem Zylinder eingeschlossenen Minimalfläche mit externen Daten, die durch eine Platte getrennt sind.

Wir beweisen, dass für beliebige externe Daten, die durch eine Platte getrennt sind, die symmetrische Teile des Zylinders enthält, ein ähnliches Verhalten wie in [8] besitzen. Die Ergebnisse zeigen, dass die Minimalfläche bei breiter Platte von den Daten getrennt wird, während eine schmale Platte eine Verbindung ermöglicht. Dies erlaubt uns, das Verhalten ähnlicher Modelle mit symmetrisch platzierten Daten vorherzusagen. Darüber hinaus zeigen die Untersuchungen, dass die Fläche bei ausreichend schmalen Platten am Zylinder “klebt”.

Schließlich präsentieren wir ein Beispiel, bei dem die Minimierer vollständig von den externen Daten getrennt sind, ein Phänomen, das nur bei nichtlokalen Minimalflächen auftritt. Diese Arbeit liefert wertvolle Erkenntnisse über das Verhalten dieser neuen mathematischen Objekte und ihre Wechselwirkung mit externen Daten.

List of symbols

Any set considered in this thesis is assumed to be Lebesgue measurable and has at least Lipschitz boundary.

\mathbb{R}^n	Euclidean space of dimension n
\mathcal{H}^n	Hausdorff measure on \mathbb{R}^n
B_r	Open ball of radius r centered at the origin
$B_r(x)$	Open ball of radius r centered at x
$B'_r(x)$	Open Ball of radius r centered at x in \mathbb{R}^{n-1}
$\text{dist}(A, B)$	Distance between sets A and B

Contents

Abstract	v
1 Introduction	1
1.1 Classical Minimal Surfaces	1
1.2 Nonlocal Minimal Surfaces	2
2 Model	7
3 Disconnected Minimizer	13
Conclusion	21
Bibliography	22

1 Introduction

Minimal surfaces - During the 18th century mathematicians like *Euler* and *Lagrange* concerned themselves with the problem of finding the set of smallest surface area given some contour, often referred to as the *Plateau Problem*. The solution of such a problem is called *Minimal Surface* and the work of Euler and Lagrange laid the foundation for the study of those. While not solving the Plateau Problem themselves, they found necessary conditions on these surfaces, namely the *Euler-Lagrange equations* [25]. Nowadays, we have multiple tools to define and characterize minimal surfaces, among those the concept known as *Perimeter*. The modern understanding of the perimeter is due to the work of *Caccioppoli* and *De Giorgi* in the 20th century [25]. Roughly speaking, the perimeter of a set can be understood as the surface area of the boundary of the set, more on that in Section 1.1. With the concept of the perimeter, we can define a minimal surface as the set which has the smallest perimeter given some external data. In modern times, minimal surfaces have found many applications, from understanding physical phenomena like soap films and black holes to informing the design of optimal structures in engineering and architecture.

In this thesis, we want to explore a rather recent concept of minimal surfaces, namely *Nonlocal Minimal Surfaces*, which were first introduced by *Cafarelli*, *Roquejoffre*, and *Savin* in 2010 [3]. For that purpose, we will first give a short introduction to the theory of minimal surfaces in the context of this work.

1.1 Classical Minimal Surfaces

The study of minimal surfaces concerns itself with finding the set of least surface area or *perimeter* under certain constraints. But before we can formulate the usual problem, we have to define some tools [7].

Definition 1.1. Let $E \subset \mathbb{R}^n$ be a set with smooth boundary, then the *perimeter* of E is given by

$$\text{Per}(E) := \sup \left\{ \int_{\partial E} \varphi \cdot \nu_E \, d\mathcal{H}^{n-1} \mid \varphi \in C_c^1(\mathbb{R}^n, \mathbb{R}^n), |\varphi| \leq 1 \right\},$$

where ν_E is the outer normal to E .

The *perimeter* of a set can be understood as the surface area of the set's boundary. An easy example would be the perimeter of a circle, which is just the circumference of the circle. To extend this definition to general measurable sets, we can use the divergence theorem and rewrite the integration over the boundary as an integration over the set itself. This removes the need for a smooth boundary and allows us to define the surface area for general sets.

Definition 1.2. Let $E \subset \mathbb{R}^n$, then the perimeter of E is given by

$$\text{Per}(E) := \sup \left\{ \int_E \text{div } \varphi \mid \varphi \in C_c^1(\mathbb{R}^n, \mathbb{R}^n), |\varphi| \leq 1 \right\}.$$

Even now, without the explicit integration over the boundary of the set, we can understand the perimeter in a sense as the surface area of the boundary. In fact, *De Giorgi* and *Federer* have shown that the perimeter of a set coincides with the $(n-1)$ -dimensional Hausdorff measure of a suitable subset of the topological boundary of the set [16]. This supports the idea that the perimeter of a set can be understood as the surface area of the set's boundary.

Usually we are interested in the minimization of the perimeter of a set relative to some external data. Thus, we need a tool which allows us to localize the area of interest.

Definition 1.3. Let $E \subset \mathbb{R}^n$ and take $\Omega \subset \mathbb{R}^n$ bounded, then the perimeter of E relative to Ω is given by

$$\text{Per}(E, \Omega) := \sup \left\{ \int_E \text{div } \varphi \mid \varphi \in C_c^1(\Omega, \mathbb{R}^n), |\varphi| \leq 1 \right\}.$$

With the necessary tools defined we can formulate the usual problem.

Definition 1.4 (Minimal Surface Problem). Let $\Omega \subset \mathbb{R}^n$ bounded and $E_0 \subset \mathbb{R}^n$, then we want to find $E \subset \mathbb{R}^n$ such that E minimizes the perimeter of E_0 relative to Ω , i.e.

$$\text{Per}(E, \Omega) = \min \{ \text{Per}(F, \Omega) \mid F \setminus \Omega = E_0 \setminus \Omega \}.$$

This set E is then called a *minimal surface*.

Note. We use the term “minimal surface” in the sense that we minimize over the area of surfaces, whereas in the context of differential geometry one sometimes uses the term “minimal surfaces” for critical points of the area functional, see [27].

For existence and other interesting properties of the classical perimeter and minimal surfaces not needed here in this work, we refer to [7], [14], [19], [20] and [25].

1.2 Nonlocal Minimal Surfaces

A standard example of a minimal surface are soap films [31]. Imagine you have a some wire, dip it in soap and observe the soap film that forms. This film is a minimal surface, i.e. it has the smallest surface area for the given contour (the wire). Observing the soap film with the naked eye, it seems like the soap film is a 2-dimensional object, see Figure 1.1, thus to minimize the area we only need to consider each point and its immediate neighborhood in the film, i.e. we only need to minimize locally¹. If we consider some set $E \subset \mathbb{R}^n$

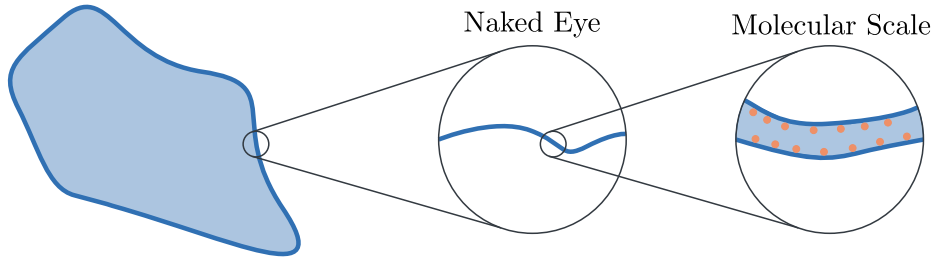


Figure 1.1 Soap film formed by a wire. Soap molecules are represented by the orange dots.

with smooth boundary, then to obtain its perimeter we have to compute

$$\int_{\partial E} \varphi \cdot \nu_E.$$

Notice that this is a local quantity, i.e. it only depends on the boundary of E . Now let us zoom in on the soap film. Zooming in on the soap film at molecular scale, we see that the soap film is a 3-dimensional object, see Figure 1.1, and the classical theory of minimal surfaces does not suffice anymore. Notice that we can no longer just minimize over the boundary of the set, but also need to minimize the volume of the set itself, thus we need to incorporate long-range correlation into the definition of the perimeter and minimal surfaces. This is where the concept of a *Fractional Perimeter* comes into play as introduced by *Cafarelli, Roquejoffre* and *Savin* in 2010 [3].

¹Refers to the proximity of a point and not the area of interest

Definition 1.5 (Fractional Perimeter). Let $E \subset \mathbb{R}^n$ be a Borel set, $s \in (0, 1)$, then the s -perimeter or fractional perimeter of E is given by

$$\text{Per}_s(E) := \int_E \int_{E^c} \frac{1}{|x - y|^{n+s}} dy dx.$$

Intuitively, we can understand the parameter s as the grade of nonlocality. Indeed, for smaller s the contribution of points further away from each other have a bigger impact on the fractional perimeter.

Corollary 1.6. The fractional perimeter is translation invariant and positive homogeneous of grade $n - s$.

Proof. Let $E \subset \mathbb{R}^n$ be a Borel set, $s \in (0, 1)$. Take any $h \in \mathbb{R}^n$, then

$$\text{Per}_s(E + h) = \int_{E+h} \int_{(E+h)^c} \frac{1}{|x - y|^{n+s}} dy dx = \int_E \int_{E^c} \frac{1}{|x - y|^{n+s}} dy dx = \text{Per}_s(E).$$

Now take any $\lambda > 0$, then

$$\text{Per}_s(\lambda E) = \int_{\lambda E} \int_{(\lambda E)^c} \frac{1}{|x - y|^{n+s}} dy dx = \int_E \int_{E^c} \frac{\lambda^{2n}}{|\lambda x - \lambda y|^{n+s}} dy dx = \lambda^{n-s} \text{Per}_s(E).$$

■

Note. Here we consider the definition of the fractional perimeter given by the authors in [4].

Other papers like [26] define a more general definition of the fractional perimeter with some nonlocal kernel $K : \mathbb{R}^n \rightarrow [0, \infty]$, $K \not\equiv \infty$

$$\text{Per}_K(E) := \int_E \int_{E^c} K(x - y) dy dx.$$

Our definition is a special case of this more general definition with the kernel $K(x) = \frac{1}{|x|^{n+s}}$.

Note. In some literature like [7], the fractional perimeter is sometimes defined with a factor 2 in front of the integral. This is just a convention to relate the fractional perimeter to the Gagliardo seminorm

$$\|f\|_{W^{s,1}(\mathbb{R}^n)} = \int_{\mathbb{R}^n} \int_{\mathbb{R}^n} \frac{|f(x) - f(y)|}{|x - y|^{n+s}} dy dx$$

to the fractional perimeter. Notice that

$$\text{Per}_s(E) = \int_E \int_{E^c} \frac{1}{|x - y|^{n+s}} dy dx = \frac{1}{2} \int_{\mathbb{R}^n} \int_{\mathbb{R}^n} \frac{|\chi_E(x) - \chi_E(y)|}{|x - y|^{n+s}} dy dx = \frac{1}{2} \|\chi_E\|_{W^{s,1}(\mathbb{R}^n)},$$

i.e. the fractional perimeter is the seminorm of the indicator function of E up to a multiplicative constant.

The fractional perimeter can be seen as a generalization of the classical perimeter. This is among other reasons due to the fact that for a set of finite classical perimeter, say E , we have that $(1 - s) \text{Per}_s(E) \rightarrow c \text{Per}(E)$ as $s \nearrow 1$ for some dimensional constant $c > 0$ [4]. Another argument for the relation between the fractional perimeter and the classical perimeter is that the fractional perimeter can be seen as the $W^{s,1}$ Gagliardo seminorm, as mentioned before. Thus, for $s \nearrow 1$ we can see the natural connection to the classical perimeter, which is in some sense the $W^{1,1}$ seminorm of χ_E [14].

Let us now consider an example where the classical perimeter does not suffice and the fractional perimeter gives us better results. The example was discussed in [6] and [31].

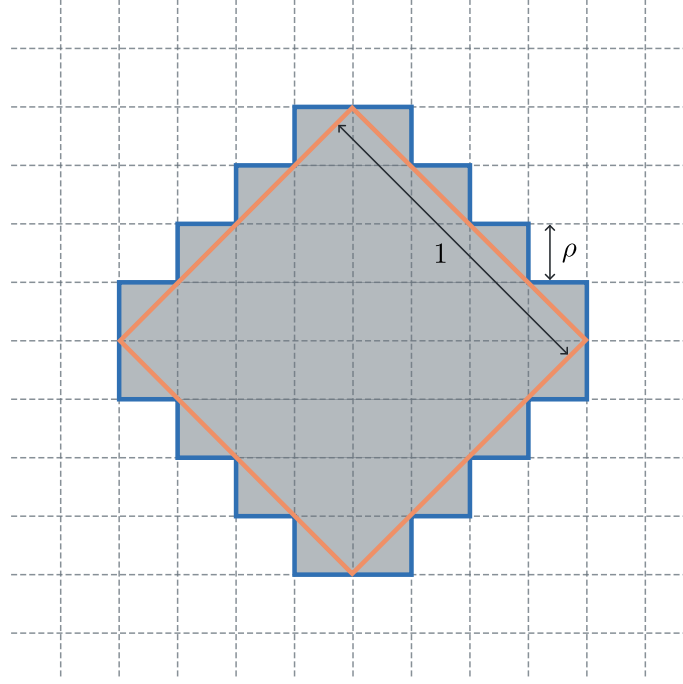


Figure 1.2 Unit square displayed by a grid of square pixels of length ρ . Orange the actual boundary of the square, Blue the boundary of the pixelated square.

Example 1.7. Consider a grid of square pixels of length ρ and a unit square rotated by 45 degrees, see Figure 1.2.

While the perimeter of the actual square is 4, the classical perimeter of the unit square composed of pixels is $4\sqrt{2}$ independent of the size of the pixels ρ . Indeed, we have that

$$\text{Per}(\text{Pixelated Square}) = 2\rho \cdot (\text{number of pixels on the boundary}) = 8\rho \cdot \frac{1}{\sqrt{2}\rho} = 4\sqrt{2}.$$

We assume that the number of pixels on the boundary is a natural number for simplicity. We see, that the classical perimeter does not suffice to capture the actual perimeter of the square accurately, even for small pixel sizes.

Now let us consider the fractional perimeter of the pixelated square. Let Q be the unit square, Q_ρ the pixelated square and $N \in \mathbb{N}$ be the number of pixels on the boundary of Q . Notice that Q_ρ is the union of Q and N disjoint isosceles triangles T_i . We then have (omit the argument for simplicity)

$$\begin{aligned} \text{Per}_s(Q_\rho) &= \int_{Q_\rho} \int_{Q_\rho^c} = \int_Q \int_{Q_\rho^c} + \int_{\cup_{i=1}^N T_i} \int_{Q_\rho^c} = \int_Q \int_{Q^c} - \int_Q \int_{\cup_{i=1}^N T_i} + \int_{\cup_{i=1}^N T_i} \int_{Q_\rho^c} \\ &= \text{Per}_s(Q) + \text{Per}_s(\cup_{i=1}^N T_i) - 2 \int_Q \int_{\cup_{i=1}^N T_i}. \end{aligned} \quad (1.1)$$

We can bound $\text{Per}_s(\cup_{i=1}^N T_i)$ from above by

$$\text{Per}_s(\cup_{i=1}^N T_i) \leq \sum_{i=1}^N \text{Per}_s(T_i) \leq \sum_{i=1}^N \rho^{2-s} \text{Per}_s(T) = N\rho^{2-s} \text{Per}_s(T) \leq c\rho^{1-s},$$

where we scaled T_i to the Triangle T with side length 1 and c is a constant. With the dominated convergence theorem we can show that the last term in (1.1) goes to 0 for $\rho \rightarrow 0$. Indeed, we have $\chi_{\cup_{i=1}^N T_i} \rightarrow 0$ a.e. for $\rho \rightarrow 0$ and $\int_Q \int_{\cup_{i=1}^N T_i} \leq \text{Per}_s(Q) < \infty$ for all ρ [29].

Thus, the discrepancy between the fractional perimeter of the pixelated square and the actual square, that is

$|\text{Per}_s(Q) - \text{Per}_s(Q_\rho)|$, behaves like $\rho^{1-s} + a(\rho)$ for some function a such that $a(\rho) \rightarrow 0$ as $\rho \rightarrow 0$. This shows that the fractional perimeter can capture the actual perimeter of the square more accurately and serves as a more robust framework than the classical perimeter in some cases.

Just as in the classical case, we can define a relative fractional perimeter by removing the integration over some constant part. We split up the domain of integration (omit the argument for simplicity)

$$\int_E \int_{E^c} = \int_{E \cap \Omega} \int_{E^c} + \int_{E \setminus \Omega} \int_{E^c} = \int_{E \cap \Omega} \int_{E^c} + \int_{E \setminus \Omega} \int_{\Omega \setminus E} + \int_{E \setminus \Omega} \int_{E^c \setminus \Omega}.$$

While minimizing E relative to Ω we can ignore the last term. Since we are only interested in the part of the minimizer E in Ω , the last term is constant and thus does not affect the minimization.

Definition 1.8. Let $A, B \subset \mathbb{R}^n$ be Borel sets, $s \in (0, 1)$, then the interaction of A and B is given by

$$\mathcal{L}(A, B) := \int_A \int_{B^c} \frac{1}{|x - y|^{n+s}} dy dx.$$

Note. In particular, we have that $\text{Per}_s(E) = \mathcal{L}(E, E^c)$.

Definition 1.9 (Relative Fractional Perimeter). Let $E \subset \mathbb{R}^n$ be a Borel set, $\Omega \subset \mathbb{R}^n$ bounded and $s \in (0, 1)$, then the s -perimeter of E relative to Ω is given by

$$\text{Per}_s(E, \Omega) := \mathcal{L}(E \cap \Omega, E^c) + \mathcal{L}(E \setminus \Omega, \Omega \setminus E).$$

With these tools we can now define the nonlocal minimal surface problem.

Definition 1.10 (Nonlocal Minimal Surface Problem). Let $\Omega \subset \mathbb{R}^n$ bounded and $E_0 \subset \mathbb{R}^n$, then we want to find $E \subset \mathbb{R}^n$ such that E minimizes the s -perimeter of E_0 relative to Ω , i.e.

$$\text{Per}_s(E, \Omega) = \min \{ \text{Per}_s(F, \Omega) \mid F \setminus \Omega = E_0 \setminus \Omega \}.$$

Over the last few years these nonlocal minimal surfaces have been an area of great interest. Various properties have been studied and numerous results have been obtained. Some of the more notable ones are a monotonicity formula, see [3], and enhanced regularity properties compared to classical minimal surfaces, see [5] and [28].

An important tool in the study of minimal surfaces are the *Euler-Lagrange equations*. These equations give us necessary conditions for a set to be a minimal surface. In the case of classical minimal surfaces these equations with the right argument are even sufficient [25]. The authors in [3] have shown that nonlocal minimal surfaces also have to satisfy a nonlocal version of the Euler-Lagrange equations in the viscosity sense.

Let $E \subset \mathbb{R}^n$ be a nonlocal minimal surface relative to some set Ω . If $E \cap \Omega$ has an interior tangent ball at some point $x \in \partial E \cap \Omega$, then

$$\int_{\mathbb{R}^n} \frac{\chi_{E^c}(y) - \chi_E(y)}{|y - x|^{n+s}} dy \geq 0.$$

Notice that this is a nonlocal version of the classical mean curvature equation given by $H_E = 0$ on ∂E , where H_E is the mean curvature on ∂E , in particular a local entity. This gives us another reason as to why we refer to *nonlocal* minimal surfaces. For further details on the Euler-Lagrange equations for minimal surfaces we refer to [3] and [25].

An interesting property unique to nonlocal minimal surfaces is the so-called *stickiness property*. With *stickiness*, we refer to the case that the boundary of the minimizer and prescribed set intersect on a measurable

set, i.e. $\mathcal{H}^{n-1}(\partial E \cap \partial \Omega) \neq 0$. While in the classical case minimal surfaces cannot stick to the boundary of the prescribed set, nonlocal minimal surfaces can stick. That is, let E be a classical minimal surface relative to some prescribed set Ω , then ∂E and $\partial \Omega$ are transverse, see [13] and [22]. In [8] the authors have given an explicit example of a nonlocal minimal surface which sticks to the boundary of the prescribed set. In this thesis we will generalize this example and show that for those models the stickiness property persists.

In this thesis, we want to explore more on these surfaces and their properties, in particular the connectedness of minimizers of certain models and the stickiness property in the same context. In Chapter 2 we will consider a generalization of the model given in [8]. In Chapter 3 we will discuss a natural question emerging while analyzing the models in Chapter 2, that is the existence of a nontrivial minimizer in the case that the external data and the prescribed set have nonzero distance. We will provide an example where such a minimizer exists. This behavior is unique to nonlocal minimal surfaces.

2 Model

In this chapter we will consider a generalization of the model considered by Dipierro et al. in [8], where they considered the external data E_0 as the complement of a slab in \mathbb{R}^n of width $2M$ and the prescribed data Ω as the cylinder of radius 1 and height $2M$. They showed that for M big enough the minimizer is disconnected which is consistent with the classical theory of minimal surfaces. When M is small enough however, the minimizer is connected and even sticks to the boundary. The latter being a unique property of nonlocal minimal surfaces.

Here we will show that for any external data E_0 such that

$$E_R := \{(x', x_n \mid |x'| < 1, M < |x_n| < M + R)\} \subset E_0 \subset \{(x', x_n \mid |x_n| > M)\}$$

and prescribed data $\Omega := \{(x', x_n \mid |x'| < 1, |x_n| < M)\}$, for some $M, R > 0$ displays the same behavior as the model considered in [8]. That is, for M big enough the minimizer is disconnected and for M small enough the minimizer is connected and sticks to the boundary.

For $n \geq 2$ consider any external data E_0 and prescribed data as above. The Figure 2.1 illustrates the setting.

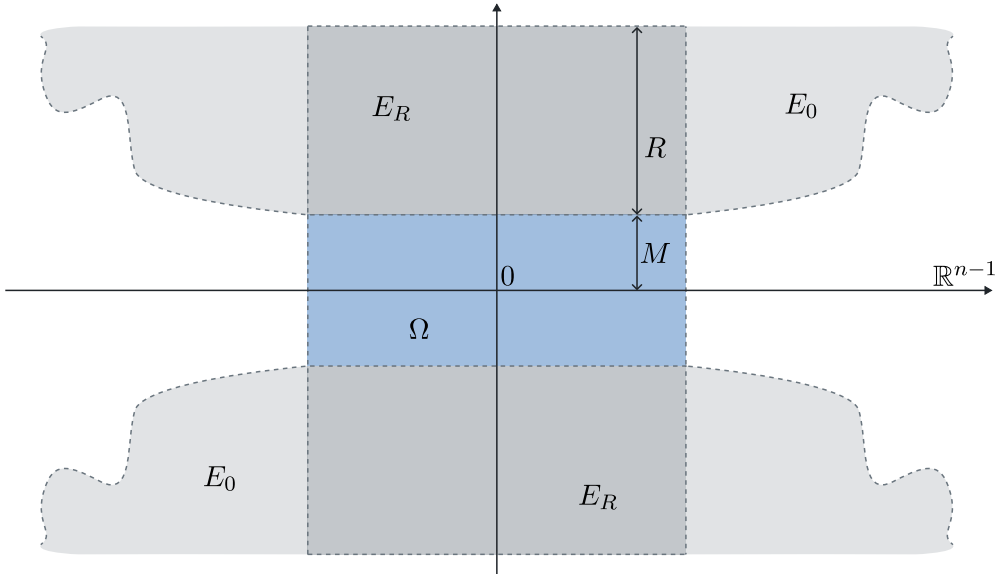


Figure 2.1 Basic setting of the model with external data E_0 and prescribed data Ω .

We state the following two results, which we will prove afterward.

Theorem 2.1. For E_0 and Ω as above and any $R > 0$ there exists an $M_0 \in (0, 1)$ depending on the dimension, R and s , such that for any $M \in (0, M_0)$ the minimizer E_M is given by $E_M = E_0 \cup \Omega$.

Theorem 2.2. For E_0 and Ω as above and any $R > 0$ there exists an $M_0 > 1$ depending on the dimension, R and s , such that for any $M > M_0$ the minimizer E_M is disconnected.

For the first proof, we will follow a similar construction as in [8].

In [3] the authors have shown that nonlocal minimizer satisfy the Euler-Lagrange equation in the viscosity

sense, i.e. if E is a minimizer, there exists some such that $q \in \partial E$ and $B_r(q + r\nu) \subset E$ for some $r > 0$ and unit vector $\nu \in \mathbb{R}^n$, then

$$\int_{\mathbb{R}^n} \frac{\chi_{E^c}(y) - \chi_E(y)}{|y - q|^{n+s}} dy \geq 0. \quad (2.1)$$

In the proof we will assume that there exist a minimizer which is not $E_0 \cup \Omega$. To bring this assumption to a contradiction, we want to show that the left-hand side of (2.1) is negative for M small enough. Thus, we have to construct some suitable ball such that we can apply the Euler-Lagrange equation. We will construct this ball by sliding a ball of some suitable radius down from e_n direction. If the minimizer is not $E_0 \cup \Omega$, then at some point the ball will touch the minimizer for any $0 < r < 1$ and a point q , then exists. Then we will split the domain into four parts and estimate each part to get the contradiction. To deal with the integration close to q we will follow the construction in [3] and reflect the ball at the touching point to cancel symmetric parts.

Proof of Theorem 2.1. Proof by contradiction. Assume the minimizer E_M is not $E_0 \cup \Omega$. Then we can slide a ball of some radius r down in e_n direction and at some point it will touch the minimizer. We consider the ball $B_r(te_n)$. Since E_M is not $E_0 \cup \Omega$, there exists $r_0 \in (0, 1)$ and $t_0 > 0$ such that $\partial B_{r_0}(t_0 e_n) \cap \partial E_M \neq \emptyset$ and $B_{r_0}(te_n) \subset E_M$ for all $t > t_0$, see Figure 2.2. In the following we define $z := t_0 e_n$.

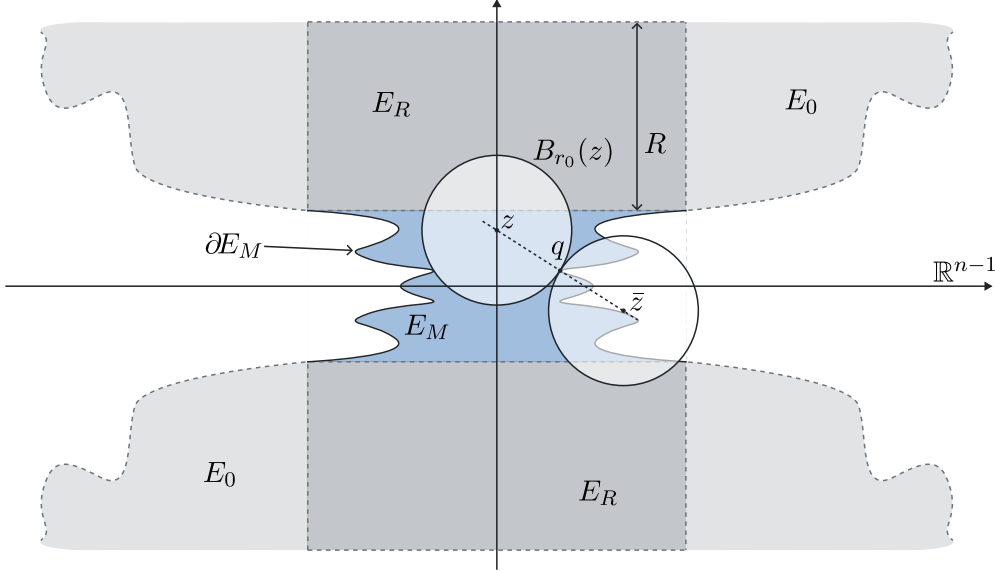


Figure 2.2 Sliding ball down and reflecting at the touching point q .

Since E_M is a minimizer it is also a viscosity solution of the Euler-Lagrange equation and the inequality

$$\int_{\mathbb{R}^n} \frac{\chi_{E_M^c}(y) - \chi_{E_M}(y)}{|y - q|^{n+s}} dy \geq 0 \quad (2.2)$$

holds, whereas $q \in \partial B_{r_0}(z) \cap \partial E_M$, since $B_{r_0}(z)$ is an interior tangent ball to E_M .

We will bring this to a contradiction by showing that the left-hand side is negative for M small enough. We will split the domain up and estimate each part.

We define the following sets, see Figure 2.3:

$$\begin{aligned} A &:= \{(x', x_n) \mid |x' - q'| < 2, |x_n - q_n| < 2M\}, \\ B &:= \{(x', x_n) \mid |x' - q'| < 2, |x_n - q_n| < R\}, \\ C &:= E_M^c \setminus B, \\ D &:= E_M \setminus A, \end{aligned}$$

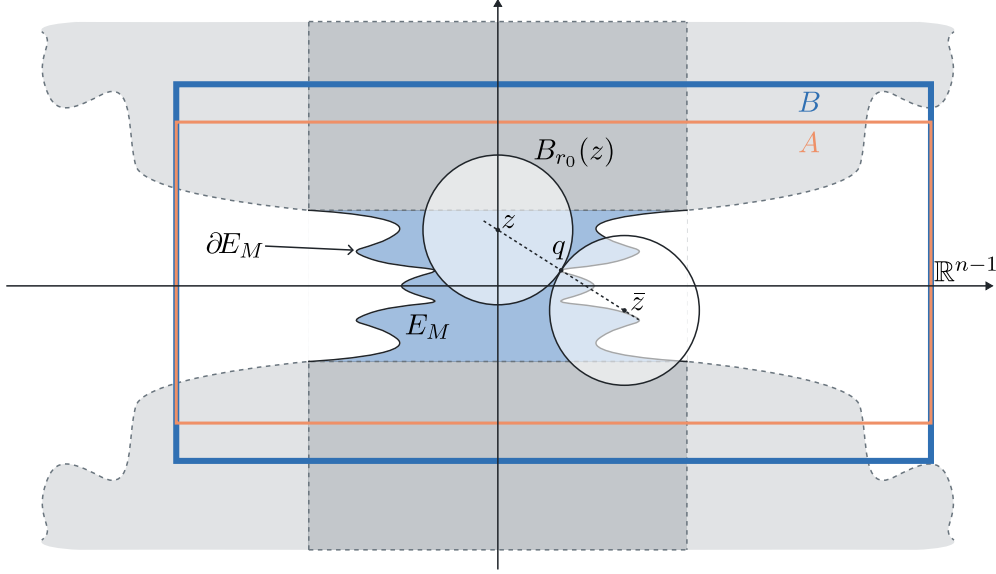


Figure 2.3 Splitting of the domain.

where R is chosen such that $E_R \subset E_0$, and we chose M such that $2M < R$ for technical reasons, which will become clear later.

First let us assume that $R \geq 2$.

We start by estimating the integral over C . Notice that $C \subset E_M^c$ and $C \subset \{|y| \geq 2\}$. Thus, we can bound

$$\int_C \frac{\chi_{E_M^c} - \chi_{E_M}}{|y - q|^{n-s}} dy = \int_C \frac{1}{|y - q|^{n-s}} dy \leq \int_{|y| \geq 2} \frac{1}{|y|^{n+s}} dy \leq c(n, s) 2^{-s},$$

where $c(n, s)$ is some positive constant depending on the dimension and the parameter s .

Next we estimate the integral over D . This part is the negative contribution of our integral, and we want it to increase as we make M smaller. First notice that $D \subset E_M$, thus the integral is negative. To get an upper bound we can restrict the domain to something smaller. We choose the ball $B_M(q + 3Me_n)$ if q_n is negative or $B_M(q - 3Me_n)$ if q_n is positive, see Figure 2.4. If needed we can also shift the ball closer to the origin by shifting it by M in $\frac{-q'}{|q'|}$ direction. Important here is that the distance between the ball and q scales with M . Finally, we multiply the integral by $\frac{1}{2}$, since it may be that not the whole ball is in D but since we chose $2M < R$ half of the ball (the part closer to q) is in D for sure. Thus, we have

$$\int_D \frac{\chi_{E_M^c} - \chi_{E_M}}{|y - q|^{n-s}} dy = - \int_D \frac{1}{|y - q|^{n-s}} dy \leq -c(n) \int_{B_M(3Me_n)} \frac{1}{|y|^{n+s}} dy \leq -c(n, s) M^{-s}.$$

Finally, we estimate the integral over the rest of the domain $S := \mathbb{R}^n \setminus (C \cup D)$. First notice that

$$\int_{S \cap B_{r_0}(q) \cap B_{r_0}(z)} \frac{1}{|y - q|^{n+s}} dy = \int_{S \cap B_{r_0}(q) \cap B_{r_0}(\bar{z})} \frac{1}{|y - q|^{n+s}} dy$$

since the argument and S are point symmetric in q . Since $B_{r_0}(z) \subset E_M$ we have that

$$\begin{aligned} & \int_{S \cap B_{r_0}(q) \cap B_{r_0}(z)} \frac{\chi_{E_M^c} - \chi_{E_M}}{|y - q|^{n+s}} dy + \int_{S \cap B_{r_0}(q) \cap B_{r_0}(\bar{z})} \frac{\chi_{E_M^c} - \chi_{E_M}}{|y - q|^{n+s}} dy \\ & \leq - \int_{S \cap B_{r_0}(q) \cap B_{r_0}(z)} \frac{1}{|y - q|^{n+s}} dy + \int_{S \cap B_{r_0}(q) \cap B_{r_0}(\bar{z})} \frac{1}{|y - q|^{n+s}} dy = 0. \end{aligned} \quad (2.3)$$

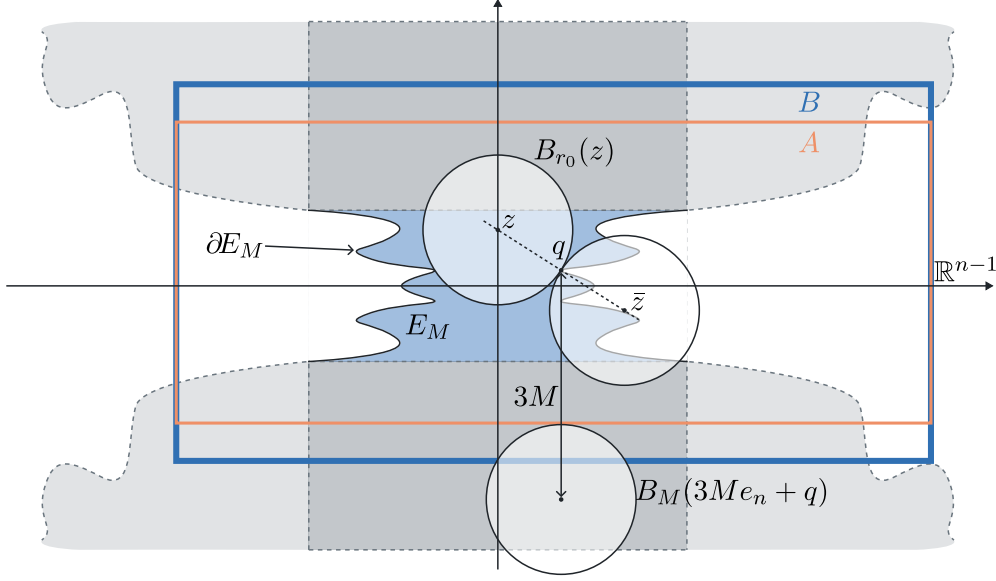


Figure 2.4 Restriction of the domain for the integral over D .

Thus, we have

$$\int_S \frac{\chi_{E_M^c} - \chi_{E_M}}{|y - q|^{n-s}} dy \stackrel{(2.3)}{\leq} \int_{S \setminus B_{r_0}(q)} \frac{1}{|y - q|^{n-s}} dy + \int_{S \cap (B_{r_0}(q) \setminus (B_{r_0}(z) \cup B_{r_0}(\bar{z})))} \frac{1}{|y - q|^{n-s}} dy. \quad (2.4)$$

For the first term we will use that $S \subset B \subset B_{R+2}$ and for the second term we will use Lemma 3.1 from [9] with the set $P_{r_0,1}$. We then get

$$\begin{aligned} (2.4) &\leq \int_{B_{R+2} \setminus B_{r_0}} \frac{1}{|y|^{n+s}} dy + \int_{P_{r_0,1}} \frac{1}{|y|^{n+s}} dy \\ &\leq c(n, s)(r_0^{-s} - (R+2)^{-s}) + c'(n, s)r_0^{-s} \\ &\leq c(n, s)(r_0^{-s} - (R+2)^{-s}). \end{aligned}$$

Since we want to contradict that $\partial B_r(te_n) \cap \partial E_M \neq \emptyset$ for all $r \in (0, 1)$ and t it is enough to consider r_0 large. Indeed, if we have that there exists some t_0 such that $\partial B_{r_0}(t_0 e_n) \cap \partial E_M \neq \emptyset$ for some r_0 , then for all $r \in (r_0, 1)$ the same holds as well. Conversely, if we have that $\partial B_{r_0}(te_n) \cap \partial E_M = \emptyset$, then for all $r \in (0, r_0)$ the same holds as well. In particular, we can choose $r_0 = 1$ (notice that we can choose $r_0 = 1$, since $B_1(z) \subset E_M$ and (2.2) still holds).

Thus, in total we have that

$$\begin{aligned} \int_{\mathbb{R}^n} \frac{\chi_{E_M^c} - \chi_{E_M}}{|y - q|^{n-s}} dy &\leq -c_0 M^{-s} + c_1(2^{-s} + 1 - (R+2)^{-s}) \\ &= -c_0 M^{-s} \left(1 - \frac{c_1}{c_0} \left(\left(\frac{M}{2} \right)^s + M^s - \left(\frac{M}{R+2} \right)^2 \right) \right). \end{aligned}$$

Now we can choose M small enough such that the right-hand side is negative. Thus, we have contradicted our assumption, that the minimizer is not $E_0 \cup \Omega$ for $R \geq 2$.

Let us now consider the case that $R < 2$, then for the integral over $C \subset \{|y| \geq R\}$ we have

$$\int_C \frac{\chi_{E_M^c} - \chi_{E_M}}{|y - q|^{n-s}} dy = \int_C \frac{1}{|y - q|^{n-s}} dy \leq \int_{|y| \geq R} \frac{1}{|y|^{n+s}} dy \leq c(n, s)R^{-s}.$$

The integral over D and S are the same as before, but this time we can't choose $r_0 = 1$ since it could be that $B_1(z) \not\subset E_M$. Still we can choose $r_0 = \frac{R}{2}$, since $B_{\frac{R}{2}}(z) \subset E_M$. Thus, we have

$$\begin{aligned} \int_{\mathbb{R}^n} \frac{\chi_{E_M^c} - \chi_{E_M}}{|y - q|^{n-s}} dy &\leq -c_0 M^{-s} + c_1 (R^{-s} + r_0^{-s} - (R+2)^{-s}) \\ &= -c_0 M^{-s} \left(1 - \frac{c_1}{c_0} \left(\left(\frac{M}{R} \right)^s + \left(\frac{2M}{R} \right)^s - \left(\frac{M}{R+2} \right)^s \right) \right). \end{aligned}$$

Again we choose M small enough such that the right-hand side is negative.

Notice that in this case we have only shown for now that the cylinder $Z_R := B'_{\frac{R}{2}} \times (-M, M)$ is part of the minimizer.

In the classical case we could conclude connectedness of the minimizer now, since we have found a cylinder which connects the external data, but as it turns out in the setting of nonlocal minimal surfaces, there still could exist some disconnected part of the minimizer. More on that in Chapter 3.

To prove that the minimizer is $E_0 \cup \Omega$ we will proceed similarly, but instead of sliding the ball down, we will push a ball outwards from inside the cylinder. Since we have shown that the cylinder Z_R is part of the minimizer, the ball $B_{\frac{R}{2}}(he_n)$ for any $h \in (-M, M)$ is part of the minimizer. We will push this ball outwards (in any direction, w.l.o.g. we can choose e_1). We assume again, that $E_M \neq E_0 \cup \Omega$, then for the ball $B_{\frac{R}{2}}((1 - \frac{R}{2} - t)e_1 + he_n)$ with $t \in (0, 1 - \frac{R}{2})$ and $h \in (-M, M)$ there exists some t_0 and h_0 such that the ball touches the minimizer, i.e. $\partial B_{\frac{R}{2}}((1 - \frac{R}{2} - t_0)e_1 + h_0e_n) \cap \partial E_M \neq \emptyset$ and for all $t \in (t_0, 1 - \frac{R}{2})$ we have that $B_{\frac{R}{2}}((1 - \frac{R}{2} - t)e_1 + h_0e_n) \subset E_M$. Again we define $z := (1 - \frac{R}{2} - t_0)e_1 + h_0e_n$.

Now we can estimate the integral again by splitting the domain. We define the following sets:

$$\begin{aligned} A &:= \{(x', x_n) \mid |x' - q'| < R, |x_n - q_n| < 2M\}, \\ B &:= \{(x', x_n) \mid |x' - q'| < R, |x_n - q_n| < R\}, \\ C &:= E_M^c \setminus B, \\ D &:= E_M \setminus A. \end{aligned}$$

The integral over C and D is estimated as before. We have that

$$\int_C \frac{\chi_{E_M^c} - \chi_{E_M}}{|y - q|^{n-s}} dy \leq \int_{|y| \geq R} \frac{1}{|y|^{n+s}} dy \leq c(n, s) R^{-s}$$

and

$$\int_D \frac{\chi_{E_M^c} - \chi_{E_M}}{|y - q|^{n-s}} dy \leq -c(n) \int_{B_M(3Me_n)} \frac{1}{|y|^{n+s}} dy \leq -c(n, s) M^{-s}.$$

For the integral over the rest of the domain S , we proceed as before. First we have again

$$\int_{S \cap B_{\frac{R}{2}}(q) \cap B_{\frac{R}{2}}(z)} \frac{1}{|y - q|^{n+s}} dy = \int_{S \cap B_{\frac{R}{2}}(q) \cap B_{\frac{R}{2}}(\bar{z})} \frac{1}{|y - q|^{n+s}} dy.$$

Thus, we have

$$\int_S \frac{\chi_{E_M^c} - \chi_{E_M}}{|y - q|^{n-s}} dy \leq \int_{S \setminus B_{\frac{R}{2}}(q)} \frac{1}{|y - q|^{n-s}} dy + \int_{S \cap (B_{\frac{R}{2}}(q) \setminus (B_{\frac{R}{2}}(z) \cup B_{\frac{R}{2}}(\bar{z})))} \frac{1}{|y - q|^{n-s}} dy. \quad (2.5)$$

For the first term we will use that $S \subset B \subset B_4$ and for the second term we will use Lemma 3.1 from [9] with the set $P_{\frac{R}{2}, 1}$. We then get

$$\begin{aligned} (2.5) &\leq \int_{B_4 \setminus B_{\frac{R}{2}}} \frac{1}{|y|^{n+s}} dy + \int_{P_{\frac{R}{2}, 1}} \frac{1}{|y|^{n+s}} dy \\ &\leq c(n, s) \left(\left(\frac{R}{2} \right)^{-s} - 4^{-s} \right) + c'(n, s) \left(\frac{R}{2} \right)^{-s} \\ &\leq c(n, s) (R^{-s} - 8^{-s}). \end{aligned}$$

Thus, in total we have that

$$\begin{aligned} \int_{\mathbb{R}^n} \frac{\chi_{E_M^c} - \chi_{E_M}}{|y - q|^{n-s}} dy &\leq -c_0 M^{-s} + c_1(r^{-s} - 8^{-s}) \\ &= -c_0 M^{-s} \left(1 - \frac{c_1}{c_0} \left(\left(\frac{M}{r} \right)^s - \left(\frac{M}{8} \right)^{-s} \right) \right). \end{aligned}$$

Thus, we can choose M small enough such that the right-hand side is negative. ■

Interesting to see, that the contribution of the external data of the same width as the prescribed set is enough to get connectedness of the minimizer and even stickiness to the boundary. Also see, that the model seems to converge to the problem, considered in [8].

Proof of Theorem 2.2. We show that for M big enough, in particular we can choose $M > 1$, the minimizer is disconnected. We will slide a ball of radius \sqrt{M} in e_1 direction and show, that this ball and the minimizer don't touch for M big enough. Assume that they are touching at some point q , then since the minimizer is a viscosity solution of the Euler-Lagrange equation, we have that

$$\int_{\mathbb{R}^n} \frac{\chi_{E_M^c} - \chi_{E_M}}{|y - q|^{n-s}} dy \leq 0. \quad (2.6)$$

Now notice that we have

$$\int_{\mathbb{R}^n} \frac{\chi_{E_M^c} - \chi_{E_M}}{|y - q|^{n-s}} dy \geq \int_{\mathbb{R}^n} \frac{\chi_{F_M^c} - \chi_{F_M}}{|y - q|^{n-s}} dy,$$

where $F_M = E_M \cup F_0$ and F_0 being the external data from the model considered in [8]. Thus, we are in the same setting as in [8] and can conclude that for M large enough the left-hand side of (2.6) is positive. Thus, we have a contradiction and the minimizer is disconnected. ■

Whereas Theorem 2.2 is consistent with the classical theory of minimal surfaces, the behavior of the minimizer in Theorem 2.1 is unique to nonlocal minimal surfaces. In [8] the authors have shown that the minimizer exhibits similar behavior as we found in Theorem 2.1 for the model considered in this chapter, however interesting to see is that even in the case of very small external data with the same width as the prescribed set the minimizer is connected and even sticks to the boundary for M small enough relative to the size of R . This suggests that the contribution of the external data E_0 above and below is enough to push the minimizer to the boundary of the prescribed set Ω .

3 Disconnected Minimizer

When discussing the connectedness of the model in Chapter 2 in the case that $R < 2$, we first just stated, that if $R < 2$ then at least the cylinder $Z_R := B'_{R/2} \times (-M, M)$ is in the minimizer. This fact is not enough for connectedness of the minimizer. To show connectedness, we would still need to show, that there cannot exist a part of the minimizer that is fully detached from the cylinder and the external data.

Motivated by the fact, that in the classical case, if we have some external data E_0 and some prescribed set Ω that are fully disconnected, i.e. $\text{dist}(E_0, \Omega) =: d > 0$, then the minimizer is the external data itself, we wanted to prove the same thing for the nonlocal case as well.

Indeed, if we could show that, then the existence of the cylinder Z_R is enough to conclude that the minimizer is connected. Assume there exists a part of the minimizer that is not connected to the cylinder and the external data, i.e. there exists a set E_1 such that $\text{dist}(E_1, E_0 \cup A) > 0$ with $A := E_M \setminus (E_0 \cup E_1)$. We can assume that A is connected and notice that $Z_R \subset A$. Then we can rewrite the fractional perimeter of $E_M := E_0 \cup A \cup E_1$ relative to Ω as follows:

$$\begin{aligned} \text{Per}_s(E_M, \Omega) &= \mathcal{L}(E_M \cap \Omega, E_M^c) + \mathcal{L}(E_M \setminus \Omega, \Omega \setminus E_M) \\ &= \mathcal{L}(E_1 \cup A, E_M^c) + \mathcal{L}(E_0, \Omega \setminus (E_1 \cup A)) \\ &= \mathcal{L}(E_1, E_M^c) + \mathcal{L}(A, E_M^c) + \mathcal{L}(E_0 \cup A, \Omega \setminus (E_1 \cup A)) - \mathcal{L}(A, \Omega \setminus (E_1 \cup A)) \\ &= \text{Per}_s(E_M, \Omega \setminus A) + \mathcal{L}(A, (E_0 \cup A)^c). \end{aligned} \quad (3.1)$$

Notice that the second term in (3.1) is now independent of E_1 , thus to minimize $\text{Per}_s(E_M, \Omega)$ we can first minimize $\mathcal{L}(A, (E_0 \cup A)^c)$ over A and then minimize $\text{Per}_s(E_M, \Omega \setminus A)$.

We define a sequence of prescribed sets $(\Omega_n)_n$ such that $\Omega_n \subset \Omega_{n+1} \subset \Omega$ and $\text{dist}(E_0 \cup A, \Omega_n) = \frac{d}{n}$, where $d := \text{dist}(E_0 \cup A, E_1)$. Then for each n we are in the situation of fully disconnected external data, here $E_0 \cup A$, and prescribed set, here Ω_n . If our assumption, that nonlocal minimizers behave like the classical minimizers for disconnected external data and prescribed set, is correct, then we could conclude

$$\text{Per}_s(E_M, \Omega \setminus A) \geq \text{Per}_s(E_M, \Omega_n) \geq \text{Per}_s(E_0, \Omega_n) \nearrow \text{Per}_s(E_0, \Omega \setminus A).$$

That is, if there exists a set E_1 fully detached from $E_0 \cup A$, then its fractional perimeter relative to Ω is larger than the fractional perimeter of $E_0 \cup A$ relative to Ω . Thus, there couldn't exist a set E_1 fully detached from $E_0 \cup Z_R$.

As it turns out, this is *not* true in general, and thus we cannot state connectedness just with the existence of the cylinder in the minimizer.

In the following, we will consider an example of a model where the external data and the prescribed set have nonzero distance, but the minimizer is not the external data itself. We will then generalize the example to arbitrary dimensions $n \geq 2$ and radii.

Example 3.1. Let $E_0 = B_2^c$ and $\Omega = B_1$ in \mathbb{R}^2 . Then we compare the fractional perimeter of E_0 relative to Ω with the fractional perimeter of $E_0 \cup \Omega$ relative to Ω , that is

$$\text{Per}_s(E_0 \cup \Omega, \Omega) - \text{Per}_s(E_0, \Omega) = \text{Per}_s(B_1) - 2L(B_2^c, B_1), \quad (3.2)$$

and show that this difference is negative for s small enough. If the difference is negative we have found a competitor to the external data with smaller fractional perimeter and thus the external data cannot be the minimizer.

For the first term we have by [21, Eq. (11)]

$$\text{Per}_s(B_1) = \frac{2^{2-s} \pi^{\frac{3}{2}} \Gamma(\frac{1-s}{2})}{s(2-s) \Gamma(\frac{2-s}{2})}.$$

We want to bound the second term from above and below. For that we will split the domain depending on x , see Figure 3.1.

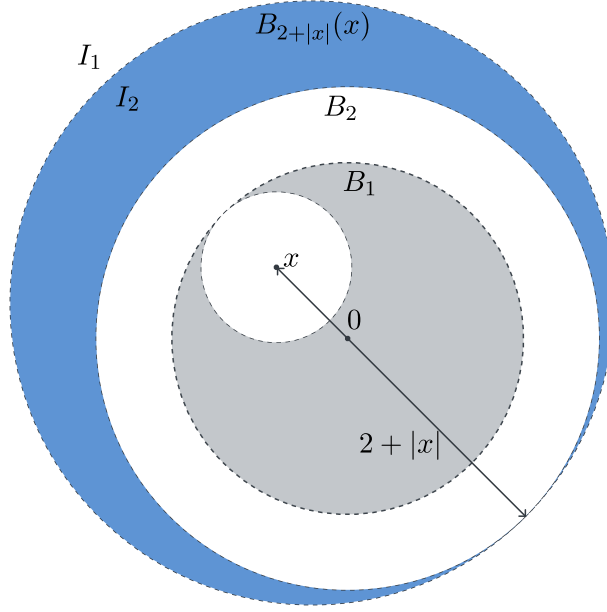


Figure 3.1 Splitting of B_2^c depending on x .

Thus, we have

$$\mathcal{L}(B_2^c, B_1) = \int_{B_1} \int_{B_2^c} \frac{1}{|x-y|^{2-s}} dy dx = \underbrace{\int_{B_1} \int_{B_{2+|x|}^c(x)} \frac{1}{|x-y|^{2-s}} dy dx}_{I_1} + \underbrace{\int_{B_1} \int_{B_{2+|x|}^c(x) \setminus B_2} \frac{1}{|x-y|^{2-s}} dy dx}_{I_2}.$$

We start with I_1 :

$$\begin{aligned} I_1 &= \int_{B_1} \int_{B_{2+|x|}^c(x)} \frac{1}{|x-y|^{2+s}} dy dx = \int_{B_1} \int_{B_{2+|x|}^c} \frac{1}{|y|^{2+s}} dy dx \\ &= 4\pi^2 \int_0^1 \int_{2+r_1}^\infty \frac{r_1}{r_2^{1+s}} dr_2 dr_1 = \frac{4\pi^2}{s} \int_0^1 \frac{r_1}{(2+r_1)^s} dr_1 \\ &= \frac{4\pi^2}{s(1-s)(2-s)} (2^{2-s} - (s+1)3^{1-s}). \end{aligned}$$

Now to I_2 . Here the idea is to use radial coordinates again. Since the integral is radial symmetric w.r.t. x , we can fix x such that $x = (r, 0)$ for $r = |x|$. Now for fixed x the domain of y is not radial symmetric, thus we first have to compute the domain of $\vartheta := \vartheta(r_1, r_2)$.

We have two restrictions on y :

$$(1) \quad 4 \leq |x-y|^2 \leq (2+2|x|)^2$$

$$(2) \quad 2 - |x| \leq |y| \leq 2 + |x|$$

From the first restriction with $|x| = r_1$, $|y| = r_2$ and ϑ the angle between x and y we get

$$\begin{aligned} 4 &\leq |x - y|^2 \leq (2 + 2r_1)^2 \\ \Leftrightarrow 4 &\leq r_1^2 + r_2^2 - 2r_1r_2 \cos(\vartheta) \leq 4(1 + r_1)^2 \\ \Leftrightarrow \frac{r_1^2 + r_2^2 - 4}{2r_1r_2} &\geq \cos(\vartheta) \geq \frac{r_1^2 + r_2^2 - 4(1 + r_1)^2}{2r_1r_2}. \end{aligned} \quad (3.3)$$

From the second restriction we have that the right-hand side of (3.3) is always greater or equal to -1 , thus we have

$$\frac{r_1^2 + r_2^2 - 4}{2r_1r_2} \geq \cos(\vartheta) \geq -1.$$

We will see, that for all r_1 and r_2 the argument of I_2 is independent of ϑ , thus we can integrate over ϑ first with $\vartheta \in D_\vartheta := \left(0, \arccos\left(\frac{r_1^2 + r_2^2 - 4}{2r_1r_2}\right)\right) \cup \left(2\pi - \arccos\left(\frac{r_1^2 + r_2^2 - 4}{2r_1r_2}\right), 2\pi\right)$

$$\int_{D_\vartheta} d\vartheta = 2\pi - 2 \arccos\left(\frac{r_1^2 + r_2^2 - 4}{2r_1r_2}\right).$$

For I_2 we can follow

$$I_2 = \int_{B_1} \int_{B_{2+|x|}(x) \setminus B_2} \frac{1}{|x - y|^{2+s}} dy dx = \int_{B_1} \underbrace{\int_{B_{2+|x|}(x) \setminus B_2(-x)} \frac{1}{|y|^{2+s}} dy}_{\text{radial symmetric w.r.t. } x} dx.$$

We use radial coordinates

$$\begin{aligned} &= 2\pi \int_0^1 \int_{2-r_1}^{2+r_1} \frac{r_1}{r_2^{1+s}} \int_{-\vartheta}^{\vartheta} d\vartheta dr_2 dr_1 = 2\pi \int_0^1 \int_{2-r_1}^{2+r_1} \frac{r_1}{r_2^{1+s}} \left(2\pi - 2 \arccos\left(\frac{r_1^2 + r_2^2 - 4}{2r_1r_2}\right)\right) dr_2 dr_1 \\ &= 4\pi^2 \int_0^1 \int_{2-r_1}^{2+r_1} \frac{r_1}{r_2^{1+s}} dr_2 dr_1 - 4\pi \int_0^1 \int_{2-r_1}^{2+r_1} \frac{r_1}{r_2^{1+s}} \arccos\left(\frac{r_1^2 + r_2^2 - 4}{2r_1r_2}\right) dr_2 dr_1, \end{aligned}$$

then partial integration

$$\begin{aligned} &= 4\pi^2 \int_0^1 \int_{2-r_1}^{2+r_1} \frac{r_1}{r_2^{1+s}} dr_2 dr_1 - \frac{4\pi^2}{s} \int_0^1 \frac{r_1}{(2-r_1)^s} dr_1 + \frac{4\pi}{s} \int_0^1 \int_{2-r_1}^{2+r_2} \frac{r_1}{r_2^{1+s}} \frac{r_2^2 - r_1^2 + 4}{\sqrt{4r_1^2r_2^2 - (r_1^2 + r_2^2 - 4)^2}} dr_2 dr_1 \\ &= \underbrace{\frac{4\pi^2}{s(1-s)(2-s)} ((s+1)3^{1-s} - 2^{2-s})}_{-I_1} + \frac{4\pi}{s} \int_0^1 \int_{2-r_1}^{2+r_2} \frac{r_1}{r_2^{1+s}} \frac{r_2^2 - r_1^2 + 4}{\sqrt{4r_1^2r_2^2 - (r_1^2 + r_2^2 - 4)^2}} dr_2 dr_1. \end{aligned}$$

Finally, we have for the second term in (3.2)

$$\mathcal{L}(E_0, E_1) = \frac{4\pi}{s} \int_0^1 \int_{2-r_1}^{2+r_2} \frac{r_1}{r_2^{1+s}} \frac{r_2^2 - r_1^2 + 4}{\sqrt{4r_1^2r_2^2 - (r_1^2 + r_2^2 - 4)^2}} dr_2 dr_1.$$

We can now bound this term without losing too much information. For the upper bound, we will use that $r_2 \geq 2 - r_1$ and for the lower bound we will use that $r_2 \leq 2 + r_1$. We then get

$$\begin{aligned} \bullet) \quad \mathcal{L}(E_0, E_1) &\leq \frac{4\pi}{s} \int_0^1 \int_{2-r_1}^{2+r_2} \frac{r_1}{(2-r_1)^s} \frac{1}{r_2} \frac{r_2^2 - r_1^2 + 4}{\sqrt{4r_1^2r_2^2 - (r_1^2 + r_2^2 - 4)^2}} dr_2 dr_1 \\ &= \frac{4\pi}{s} \int_0^1 \frac{r_1}{(2-r_1)^s} \left[\arccos\left(\frac{r_1^2 + r_2^2 - 4}{2r_1r_2}\right) \right]_{2-r_1}^{2+r_2} dr_1 \\ &= \frac{4\pi^2}{s(1-s)(2-s)} (2^{2-s} - 3 + s), \end{aligned}$$

and

$$\begin{aligned} \bullet) \quad \mathcal{L}(E_0, E_1) &\geq \frac{4\pi}{s} \int_0^1 \int_{2-r_1}^{2+r_2} \frac{r_1}{(2+r_1)^s} \frac{1}{r_2} \frac{r_2^2 - r_1^2 + 4}{\sqrt{4r_1^2 r_2^2 - (r_1^2 + r_2^2 - 4)^2}} dr_2 dr_1 \\ &= \frac{4\pi^2}{s(1-s)(2-s)} (2^{2-s} - (s+1)3^{1-s}). \end{aligned}$$

Thus, we have the bounds for (3.2)

$$\text{Per}_s(E_1) - 2\mathcal{L}(E_0, E_1) \leq \frac{2^{2-s}\pi^{\frac{3}{2}}\Gamma(\frac{1-s}{2})}{s(2-s)\Gamma(\frac{2-s}{2})} - \frac{8\pi^2}{s(1-s)(2-s)} (2^{2-s} - (s+1)3^{1-s}), \quad (3.4)$$

and

$$\text{Per}_s(E_1) - 2\mathcal{L}(E_0, E_1) \geq \frac{2^{2-s}\pi^{\frac{3}{2}}\Gamma(\frac{1-s}{2})}{s(2-s)\Gamma(\frac{2-s}{2})} - \frac{8\pi^2}{s(1-s)(2-s)} (2^{2-s} - 3 + s). \quad (3.5)$$

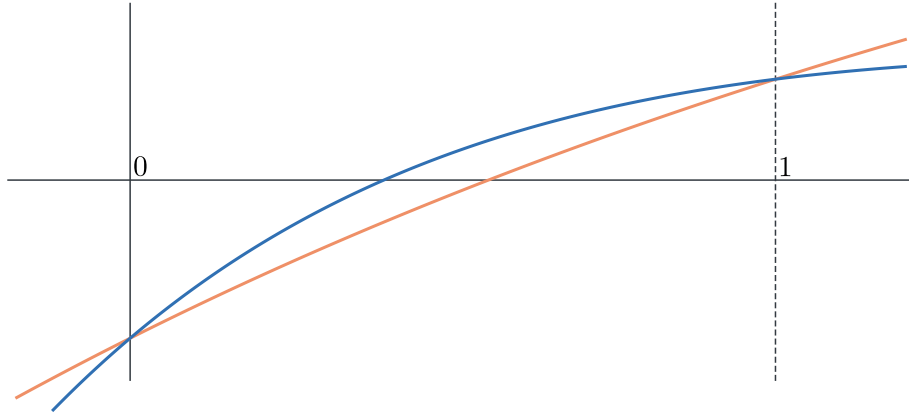


Figure 3.2 Upper and lower bound plotted for $s \in (0, 1)$.

Example 3.2 (Continuation of Example 3.1). Let us now consider the same setting as in Example 3.1, but instead with the external data $E_0 = B_{2+T} \setminus B_2$ for $T > 0$ large enough. Notice, that this change just adds one additional term compared to before

$$\mathcal{L}(B_{2+T} \setminus B_2, B_1) = \mathcal{L}(B_2^c, B_1) - \underbrace{\int_{B_{2+T}^c} \int_{B_1} \frac{1}{|x-y|^{2-s}} dx dy}_{I_3}$$

We will bound I_3 from above and below.

The upper bound

$$\begin{aligned} \int_{B_1} \int_{B_{2+T-|x|}^c(x)} \frac{1}{|x-y|^{2-s}} dy dx &\leq 4\pi^2 \int_0^1 \int_{2+T-r_1}^\infty \frac{r_1}{r_2^{1-s}} dr_2 dr_1 \\ &= \frac{4\pi^2}{s} \int_0^1 \frac{r_1}{(2+T-r_1)^s} dr_1 \\ &= \frac{4\pi^2}{s(1-s)(2-s)} [(2+T)^{2-s} - (3-s+T)(1+T)^{1-s}] \end{aligned}$$

and the lower bound

$$\begin{aligned}
\int_{B_1} \int_{B_{2+T+|x|}^c(x)} \frac{1}{|x-y|^{2-s}} dy dx &\geq 4\pi^2 \int_0^1 \int_{2+T+r_1}^{2+T+r_1} \frac{r_1}{r_2^{1-s}} dr_2 dr_1 \\
&= \frac{4\pi^2}{s} \int_0^1 \frac{r_1}{(2+T+r_1)^s} dr_1 \\
&= \frac{4\pi^2}{s(1-s)(2-s)} [(2+T)^{2-s} - (1+s+T)(3+T)^{1-s}].
\end{aligned}$$

Thus, we have the bounds

$$\text{Per}_s(E_0 \cup \Omega, \Omega) - \text{Per}_s(E_0, \Omega) \leq (3.4) + \frac{8\pi^2}{s(1-s)(2-s)} [(2+T)^{2-s} - (3-s+T)(1+T)^{1-s}],$$

and

$$\text{Per}_s(E_0 \cup \Omega, \Omega) - \text{Per}_s(E_0, \Omega) \geq (3.5) + \frac{8\pi^2}{s(1-s)(2-s)} [(2+T)^{2-s} - (1+s+T)(3+T)^{1-s}].$$

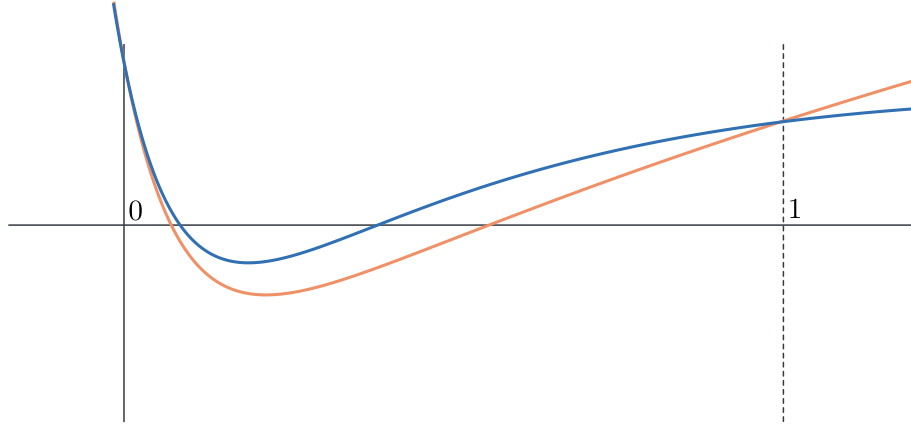


Figure 3.3 Upper and lower bound plotted for $s \in (0, 1)$ for $T = 50000$.

We now want to generalize this example to arbitrary dimensions $n \geq 2$ and radii $0 < r < R$. We will consider the following setting once with unbounded data and once with bounded data: Let $n \geq 2$ and $r, R, T > 0$, such that $r < R$. Take the external data $E_0 = B_R^c$ in the unbounded case and $E_0 = B_{R+T} \setminus B_R$ in the bounded case and define the prescribed set $\Omega = B_r$.

In [4] the authors have shown that for $s \nearrow 1$ the fractional perimeter behaves like the classical perimeter. Thus, we can expect that for s large enough the minimizer should be the external data itself. In [12] the authors have shown that for bounded sets, say A and B , the interaction multiplied with s goes to zero as $s \searrow 0$, that is $s \mathcal{L}(A, B) \rightarrow 0$ as $s \searrow 0$, see [12, Eq. (3.2)].

Theorem 3.3. Let $n \geq 2$ and $0 < r < R$. Let $E_0 = B_R^c$ and $\Omega = B_r$, then there exists an $s_0 \in (0, 1)$ such that for all $s \in (0, s_0)$ the minimizer is not the external data E_0 itself.

Theorem 3.4. Let $n \geq 2$ and $0 < r < R$ and $T > 0$. Let $E_0 = B_{R+T} \setminus B_R$ and $\Omega = B_r$, then for any T large enough there exists $s_0, s_1 \in (0, 1)$ such that for all $s \in (s_0, s_1)$ the minimizer is not the external data E_0 itself.

Proof of Theorem 3.3. As in Example 3.1 and Example 3.2 we will compare the fractional perimeter of $E_0 \cup \Omega$ relative to Ω with the fractional perimeter of E_0 relative to Ω

$$\text{Per}_s(E_0 \cup \Omega, \Omega) - \text{Per}_s(E_0, \Omega) = \text{Per}_s(\Omega) - 2\mathcal{L}(E_0, \Omega) = \text{Per}_s(B_r) - 2\mathcal{L}(B_R^c, B_r). \quad (3.6)$$

For the first term we have by [21, Eq. (11)]

$$\text{Per}_s(B_r) = \frac{2^{1-s} \pi^{\frac{n-1}{2}} n \omega_n}{s(n-s)} \frac{\Gamma(\frac{1-s}{2})}{\Gamma(\frac{n-s}{2})} r^{n-s} = \frac{2^{2-s} \pi^{n-\frac{1}{2}}}{s(n-s)} \frac{\Gamma(\frac{1-s}{2})}{\Gamma(\frac{n-s}{2}) \Gamma(\frac{n}{2})} r^{n-s}$$

with $\omega_n = \frac{\pi^{\frac{n}{2}}}{\Gamma(\frac{n}{2}+1)}$ and where Γ is the gamma function.

The second term we will bound from below to get an upper bound for (3.6).

$$\begin{aligned} \mathcal{L}(B_r, B_R^c) &= \int_{B_r} \int_{B_R^c} \frac{1}{|x-y|^{n-s}} dy dx \geq \int_{B_r} \int_{B_{R+|x|}^c(x)} \frac{1}{|x-y|^{n+s}} dy dx \\ &= \int_{B_r} \int_{B_{R+|x|}^c} \frac{1}{|y|^{n+s}} dy dx = \frac{4\pi^n}{(\Gamma(\frac{n}{2}))^2} \int_0^r \int_{R+r_1}^\infty \frac{r_1^{n-1}}{r_2^{1+s}} dr_2 dr_1 \\ &= \frac{4\pi^n}{(\Gamma(\frac{n}{2}))^2} \frac{1}{s} \int_0^r \frac{r_1^{n-1}}{(R+r_1)^s} dr_1 \\ &= \frac{4\pi^n}{(\Gamma(\frac{n}{2}))^2} \frac{1}{ns} \frac{r^{n-1}}{R^s} {}_2F_1\left(s, n; n+1; -\frac{r}{R}\right). \end{aligned}$$

In the last step we used the following identity [2] for the hypergeometric function

$$B(b, c-b) {}_2F_1(a, b; c; z) = \int_0^1 t^{b-1} (1-t)^{c-b-1} (1-tz)^{-a} dt \quad \text{for } \text{Re}(c) > \text{Re}(b) > 0,$$

where B is the beta function. In our case we have $a = s$, $b = n$, $c = n+1$ and $z = -\frac{r}{R}$, thus

$$\begin{aligned} \int_0^r \frac{r_1^{n-1}}{(R+r_1)^s} dr_1 &= \frac{r^n}{R^s} \int_0^1 r_1^{n-1} \left(1 + \frac{r}{R} r_1\right)^{-s} dr_1 \\ &= \frac{r^n}{R^s} B(n, 1) {}_2F_1\left(s, n; n+1; -\frac{r}{R}\right) = \frac{r^n}{nR^s} {}_2F_1\left(s, n; n+1; -\frac{r}{R}\right). \end{aligned}$$

Thus, we can bound (3.6) from above by

$$\begin{aligned} &\text{Per}_s(E_0 \cup \Omega, \Omega) - \text{Per}_s(E_0, \Omega) \\ &\leq \frac{2^{2-s} \pi^{n-\frac{1}{2}}}{s(n-s)} \frac{\Gamma(\frac{1-s}{2})}{\Gamma(\frac{n-s}{2}) \Gamma(\frac{n}{2})} r^{n-s} - \frac{8\pi^n}{(\Gamma(\frac{n}{2}))^2} \frac{r^n}{snR^s} {}_2F_1\left(s, n; n+1; -\frac{r}{R}\right). \end{aligned} \quad (3.7)$$

Since we are interested in the behavior of (3.6) depending on s we multiply (3.7) by $s(1-s)$ to deal with the singularities at $s = 0$ and $s = 1$

$$\begin{aligned} &s(1-s)(\text{Per}_s(E_0 \cup \Omega, \Omega) - \text{Per}_s(E_0, \Omega)) \\ &\leq \frac{2^{3-s} \pi^{n-\frac{1}{2}}}{n-s} \frac{\Gamma(\frac{3-s}{2})}{\Gamma(\frac{n-s}{2}) \Gamma(\frac{n}{2})} r^{n-s} - \frac{8\pi^n}{(\Gamma(\frac{n}{2}))^2} \frac{r^n}{nR^s} (1-s) {}_2F_1\left(s, n; n+1; -\frac{r}{R}\right). \end{aligned} \quad (3.8)$$

Since Γ is continuous for all positive reals and ${}_2F_1$ is absolutely continuous for $|z| < 1$ [2], the right-hand side of (3.8) is continuous for all $s \in (0, 1)$. First notice that we have the following limits

$$\lim_{s \searrow 0} {}_2F_1(s, n; n+1; z) = 1 \quad \text{and} \quad \lim_{s \nearrow 1} (1-s) {}_2F_1(s, n; n+1; z) = 0,$$

since for $|z| < 1$ the hypergeometric function has the following expression

$${}_2F_1(a, b; c; z) = \sum_{k=0}^{\infty} \frac{(a)_k (b)_k}{(c)_k} \frac{z^k}{k!},$$

for $(q)_k = q(q+1) \dots (q+k-1)$ and $(q)_0 = 1$ whenever $q > 0$.

Now take the limit for $s \searrow 0$ and $s \nearrow 1$ in (3.8)

$$\lim_{s \searrow 0} s(1-s)(\text{Per}_s(E_0 \cup \Omega, \Omega) - \text{Per}_s(E_0, \Omega)) = -\frac{4\pi^n}{n} \frac{1}{(\Gamma(\frac{n}{2}))^2} r^n < 0$$

and

$$\lim_{s \nearrow 1} s(1-s)(\text{Per}_s(E_0 \cup \Omega, \Omega) - \text{Per}_s(E_0, \Omega)) = \frac{4\pi^{n-\frac{1}{2}}}{n-1} \frac{1}{\Gamma(\frac{n-1}{2})\Gamma(\frac{n}{2})} r^{n-1} > 0. \quad (3.9)$$

Now we know for $s \nearrow 1$ that $(1-s) \text{Per}_s(E, \Omega)$ is approaching the classical perimeter whenever the classical perimeter is finite, thus in (3.9) is actually an equality. Thus, we can conclude that there exists an $s_0 \in (0, 1)$ such that for all $s \in (0, s_0)$ the minimizer is not the external data itself. ■

Proof of Theorem 3.4. We consider again the difference

$$\begin{aligned} \text{Per}_s(E_0 \cup \Omega, \Omega) - \text{Per}_s(E_0, \Omega) &= \text{Per}_s(\Omega) - 2\mathcal{L}(E_0, \Omega) \\ &= \text{Per}_s(B_r) - 2\mathcal{L}(B_R^c, B_r) + 2\mathcal{L}(B_{R+T}^c, B_r). \end{aligned} \quad (3.10)$$

We can use the upper bound from the proof of Theorem 3.3 for the first 2 terms in (3.10). The third term we will bound from above

$$\begin{aligned} \mathcal{L}(B_{R+T}^c, B_r) &= \int_{B_r} \int_{B_{R+T}^c} \frac{1}{|x-y|^{n-s}} dy dx \leq \int_{B_r} \int_{B_{R+T-|x|}^c} \frac{1}{|x-y|^{n-s}} dy dx \\ &= \frac{4\pi^n}{(\Gamma(\frac{n}{2}))^2} \int_0^r \int_{R+T-r_1}^{\infty} \frac{r_1^{n-1}}{r_2^{1+s}} dr_2 dr_1 = \frac{4\pi^n}{(\Gamma(\frac{n}{2}))^2} \frac{1}{s} \int_0^r \frac{r_1^{n-1}}{(R+T-r_1)^s} dr_1 \\ &= \frac{4\pi^n}{(\Gamma(\frac{n}{2}))^2} \frac{1}{ns} \frac{r^n}{(R+T)^s} {}_2F_1\left(s, n; n+1; -\frac{r}{R+T}\right). \end{aligned}$$

Thus, we can bound (3.10) from above by

$$\text{Per}_s(E_0 \cup \Omega, \Omega) - \text{Per}_s(E_0, \Omega) \leq (3.7) + \frac{8\pi^n}{(\Gamma(\frac{n}{2}))^2} \frac{1}{ns} \frac{r^n}{(R+T)^s} {}_2F_1\left(s, n; n+1; -\frac{r}{R+T}\right) \quad (3.11)$$

Now we multiply by $s(1-s)$ again to deal with the singularities at $s = 0$, $s = 1$ and take the limits

$$\lim_{s \searrow 0} s(1-s)(\text{Per}_s(E_0 \cup \Omega, \Omega) - \text{Per}_s(E_0, \Omega)) = \frac{4\pi^n}{n} \frac{1}{(\Gamma(\frac{n}{2}))^2} r^n > 0,$$

and

$$\lim_{s \nearrow 1} s(1-s)(\text{Per}_s(E_0 \cup \Omega, \Omega) - \text{Per}_s(E_0, \Omega)) = \frac{4\pi^{n-\frac{1}{2}}}{n-1} \frac{1}{\Gamma(\frac{n-1}{2})\Gamma(\frac{n}{2})} r^{n-1} > 0.$$

Notice, that the limits are independent of R and T . Also, both limits are positive. Nonetheless, for T big enough, there will exist some interval in $(0, 1)$ such that the difference is negative.

The upper bound (3.11) is continuous in T for all $s \in (0, 1)$ and for $T \rightarrow \infty$ the third term vanishes. Thus, the upper bound converges pointwise to the upper bound in the proof of Theorem 3.3. Thus, for T big enough there exists some $s \in (0, 1)$ such that the difference is negative.

The limit for $s \searrow 0$ is independent of T , positive and by [12, Eq. (3.2)] we have that $s \mathcal{L}(B_{R+T} \setminus B_R, B_r) \rightarrow 0$ for $s \searrow 0$, thus the limits in $s = 0$ and $s = 1$ are not only upper bounds but exact values.

Thus, we can conclude, that there exists an interval (s_0, s_1) such that for all $s \in (s_0, s_1)$ the minimizer is not the external data itself. ■

When comparing both theorems and their proofs, we notice that the example with bounded external data doesn't seem to converge to the example of unbounded external data, at least in the limit for $s \searrow 0$. This is interesting, as this entails, that if we want to analyze the limiting behavior of a minimizer for $s \searrow 0$ we cannot restrict the boundary data to be bounded or unbounded as the behavior might be different.

In conclusion, if we are in the setting of having external data E_0 and prescribed set Ω with nonzero distance, then we cannot assume the minimizer to be the external data. Whereas for classical minimal surfaces we can do that, nonlocal minimal surfaces can generate mass completely disconnected from its external data. Since for $s \nearrow 1$ the fractional perimeter behaves like the classical perimeter, we can at least say that for s close to 1 the minimizer will be the external data. Additionally, if we have bounded set E_0 and Ω then by the work of the authors of [12] we can conclude the same. However, for general $s \in (0, 1)$ we cannot do the same.

Nonetheless, we suspect that for E_0 and Ω with zero distance, that there exists no connected component E_1 part of the minimizer such that E_1 has nonzero distance from E_0 . This conjecture is based on the idea, that for two sets of the same size, the one connected to either E_0 or Ω will expose less surface area than the one connected to neither and thus will have a smaller fractional perimeter relative to Ω .

Conclusion

After starting with a short introduction to the classical minimal surfaces theory, we introduced the recent concept of nonlocal minimal surfaces. We presented the fractional perimeter, a generalization of the classical perimeter incorporating long-range correlations. We considered a generalization of the model considered in [8] and showed that the minimizer exhibits similar behavior depending on the width of the slab.

In the last part of the thesis, we gave an example of a model where the external data and prescribed set are disconnected, but the minimizer is not the external data itself. This is a property unique to nonlocal minimizers.

While a lot of properties of nonlocal minimizers have been studied, there are still many open questions. Here we showed that for models such as considered in Chapter 2, the minimizer changes topology depending on the width of the slab, but we don't know when and how this happens. A promising approach would be a barrier construction as shown in [12]. Another interesting question is whether there exists s_0 such that the minimizer is not the external data for all models such that the external data is unbounded and the distance between the external data and prescribed set is nonzero.

Bibliography

- [1] L. Ambrosio, G. D. Philippis, and L. Martinazzi. “Gamma-convergence of nonlocal perimeter functionals”. In: *Manuscripta Mathematica* 134.3–4 (Oct. 2010), 377–403. DOI: 10.1007/s00229-010-0399-4.
- [2] H. Bateman and B. M. Project. *Higher Transcendental Functions [Volumes I-III]*. McGraw-Hill Book Company, Aug. 2023.
- [3] L. Caffarelli, J. Roquejoffre, and O. Savin. “Nonlocal Minimal Surfaces”. In: *Communications on Pure and Applied Mathematics* 63 (Sept. 2010). DOI: 10.1002/cpa.20331.
- [4] L. Caffarelli and E. Valdinoci. “Uniform estimates and limiting arguments for nonlocal minimal surfaces”. In: *Calculus of Variations and Partial Differential Equations* 41.1 (2011), pp. 203–240. DOI: 10.1007/s00526-010-0359-6.
- [5] M. Caselli, E. Florit-Simon, and J. Serra. *Yau’s conjecture for nonlocal minimal surfaces*. 2024. DOI: 10.48550/arxiv.2306.07100.
- [6] E. Cinti, J. Serra, and E. Valdinoci. “Quantitative flatness results and BV -estimates for stable nonlocal minimal surfaces”. In: *Journal of Differential Geometry* 112 (Feb. 2016). DOI: 10.4310/jdg/1563242471.
- [7] M. Cozzi and A. Figalli. “Regularity Theory for Local and Nonlocal Minimal Surfaces: An Overview”. In: *Nonlocal and Nonlinear Diffusions and Interactions: New Methods and Directions: Cetraro, Italy 2016*. Springer International Publishing, 2017, pp. 117–158. DOI: 10.1007/978-3-319-61494-6_3.
- [8] S. Dipierro, F. Onoue, and E. Valdinoci. “(Dis)connectedness of nonlocal minimal surfaces in a cylinder and a stickiness property”. In: *Proceedings of the American Mathematical Society* (Feb. 2022). DOI: 10.1090/proc/15796.
- [9] S. Dipierro, O. Savin, and E. Valdinoci. “Graph properties for nonlocal minimal surfaces”. In: *Calculus of Variations and Partial Differential Equations* 55 (June 2016). DOI: 10.1007/s00526-016-1020-9.
- [10] S. Dipierro, O. Savin, and E. Valdinoci. “Boundary behavior of nonlocal minimal surfaces”. In: *Journal of Functional Analysis* 272.5 (2017), pp. 1791–1851. DOI: 10.1016/j.jfa.2016.11.016.
- [11] S. Dipierro, O. Savin, and E. Valdinoci. *A strict maximum principle for nonlocal minimal surfaces*. 2023. DOI: 10.48550/arxiv.2308.01697.
- [12] S. Dipierro et al. “Asymptotics of the s -perimeter as $s \searrow 0$ ”. In: *Discrete and Continuous Dynamical Systems* 33 (July 2013), pp. 2777–2790. DOI: 10.3934/dcds.2013.33.2777.
- [13] F. Duzaar and K. Steffen. “Optimal Interior and Boundary Regularity for Almost Minimizers to Elliptic Variational Integrals”. In: *Journal für die Reine und Angewandte Mathematik* 2002 (May 2000). DOI: 10.1515/crll.2002.046.
- [14] L. C. Evans and R. F. Gariepy. *Measure Theory and Fine Properties of Functions, Revised Edition*. Boca Raton, Fla: CRC Press, 2015. ISBN: 978-1-482-24239-3.
- [15] A. Figalli et al. “Isoperimetry and Stability Properties of Balls with Respect to Nonlocal Energies”. In: *Communications in Mathematical Physics* 336.1 (Dec. 2014), 441–507. DOI: 10.1007/s00220-014-2244-1.
- [16] W. Fleming. “Early developments in geometric measure theory”. In: *Indiana University Mathematics Journal* 69 (Jan. 2020), pp. 173–204. DOI: 10.1512/iumj.2020.69.8229.
- [17] R. Frank, E. Lieb, and R. Seiringer. “Hardy-Lieb-Thirring inequalities for fractional Schrodinger operators”. In: *Journal of the American Mathematical Society* 21 (Nov. 2006). DOI: 10.1090/S0894-0347-07-00582-6.

- [18] N. Fusco, V. Millot, and M. Morini. “A quantitative isoperimetric inequality for fractional perimeters”. In: *Journal of Functional Analysis* (Aug. 2011), pp. 697–715. DOI: 10.1016/j.jfa.2011.02.012.
- [19] E. Giusti. *Minimal Surfaces and Functions of Bounded Variation*. Birkhäuser Boston, 1984. DOI: 10.1007/978-1-4684-9486-0.
- [20] P. Grinfeld. *Introduction to Tensor Analysis and the Calculus of Moving Surfaces*. Springer New York, 2013. DOI: 10.1007/978-1-4614-7867-6.
- [21] J. Haddad and M. Ludwig. *Affine Fractional Sobolev and Isoperimetric Inequalities*. 2022. DOI: 10.48550/arxiv.2207.06375.
- [22] R. Hardt and L. Simon. “Boundary Regularity and Embedded Solutions for the Oriented Plateau Problem”. In: *Bulletin of The American Mathematical Society* 1 (Nov. 1979). DOI: 10.1090/S0273-0979-1979-14581-6.
- [23] L. Lombardini. “Approximation of sets of finite fractional perimeter by smooth sets and comparison of local and global s -minimal surfaces”. In: *Interfaces and Free Boundaries* 20 (Dec. 2016). DOI: 10.4171/ifb/402.
- [24] M. Ludwig. “Anisotropic fractional perimeters”. In: *Journal of Differential Geometry* 96.1 (Jan. 2014). DOI: 10.4310/jdg/1391192693.
- [25] F. Maggi. *Sets of Finite Perimeter and Geometric Variational Problems: An Introduction to Geometric Measure Theory*. Cambridge Studies in Advanced Mathematics. Cambridge University Press, 2012. DOI: 10.1017/cbo9781139108133.
- [26] J. Mazon, J. Rossi, and J. Toledo. “Nonlocal perimeter, curvature and minimal surfaces for measurable sets”. In: *Journal d’Analyse Mathématique* 138 (July 2019). DOI: 10.1007/s11854-019-0027-5.
- [27] W. Meeks and J. Pérez. *A Survey on Classical Minimal Surface Theory*. University lecture series. American Mathematical Society, 2012. ISBN: 9780821869123.
- [28] V. Millot, Y. Sire, and K. Wang. “Asymptotics for the Fractional Allen–Cahn Equation and Stationary Nonlocal Minimal Surfaces”. In: *Archive for Rational Mechanics and Analysis* 231 (Feb. 2019). DOI: 10.1007/s00205-018-1296-3.
- [29] F. Onoue. “Some Variational Problems Involving Nonlocal Perimeters and Applications”. Scuola Normale Superiore, 2022.
- [30] A. Ponce and D. Spector. “A boxing Inequality for the fractional perimeter”. In: *Annali Scuola Normale Superiore - Classe di Scienze* (Mar. 2020), 107–141. DOI: 10.2422/2036-2145.201711_012.
- [31] J. Serra. “Nonlocal minimal surfaces: recent developments, applications, and future directions”. In: *SeMA Journal* (2023). DOI: 10.1007/s40324-023-00345-1.
- [32] E. Valdinoci, C. Bucur, and L. Lombardini. “Complete stickiness of nonlocal minimal surfaces for small values of the fractional parameter”. In: *Ann. Inst. H. Poincaré Anal. Non Linéaire* 36.3 (2019), pp. 655–703. DOI: 10.1016/j.anihpc.2018.08.003.